Supplemental Figure legends

Supplemental note (to accompany Figure 1)

Fig. 1A shows that induction of ^{bio}Ub does not alter the size of the total ubiquitin pool, implying that ^{bio}Ub probably represents a small fraction of the total cellular pool of ubiquitin. However we found that it was not possible to estimate accurately the size of this fraction since (i) our ubiquitin antibodies do not efficiently recognize free ubiquitin (and FK2 does not recognise it at all) and (ii) the difference in migration of ^{bio}Ub and Ub is very small. However we found it possible, using an antibody against histone H2A (which has a prominent mono-ubiquitinated species present in cell extracts), to distinguish mono-ubiquitinated and mono-^{bio}Ubiquitinated H2A. The H2A blot shown in Supplemental Figure S1A allows us to estimate that not more than 10% of the total pool of mono-ubiquitinated H2A carries a biotin tag.

Next, we investigated what fraction of polyubiquitinated substrates we would purify via our ^{bio}Ub pulldown procedure. Theoretical calculation of the percentage of ubiquitin conjugates that would incorporate at least one ^{bio}Ub, assuming that ^{bio}Ub represents 10% of the total pool of ubiquitin, and an average chain length of 10 ubiquitins in polyubiquitinated conjugates, predicted 60-70% of conjugates should contain a biotin tag (data not shown). We tested this prediction by comparing input and unbound fractions from cell lysates expressing ^{bio}Ub and subjected to Neutravidin pulldown, using a ubiquitin antibody (immunoblot shown in Fig. 1B). We found very little depletion of free ubiquitin, as expected given the low presence of ^{bio}Ub in the total pool of cellular ubiquitin, and approximately 50% depletion of high MW ubiquitin conjugates, in line with our estimate of 10% ^{bio}Ub in the total pool.

Figure S1 (to accompany Figure 1)

A $^{bio}Ub_6$–BirA cells were induced (or not) by tet withdrawal for 24 hours and then treated (or not) for 1 hour with MG132 before harvesting. Extracts were blotted sequentially with antibodies against Histone H2A (a prominent mono-ubiquitinated protein) and biotin. Mono-ubiquitinated H2A (Ub-H2A) is visible as a strong band migrating at around 24kDa, ^{bio}Ub-H2A is faintly visible in the induced sample (middle lane) as a slightly slower migrating band. ^{bio}Ub-H2A and Ub-H2A both disappear following MG132 treatment, indicating that ^{bio}Ub is processed by the UPS like the endogenous pool of ubiquitin.

B U2OS tet-off cell lines expressing BirA alone for control pulldowns with Neutravidin

(see Fig. 1F) were generated as described in Experimental Procedures and tested by immunoblot for expression levels of BirA. Clone 3 was selected as our control line, expressing slightly higher levels of BirA than ^{bio}Ub cells.

Figure S2 (to accompany Figure 2)

A Venn diagram of hits identified from mitotic fractions, with all 470 ^{bio}Ub-specific hits shown. A simplified version of this diagram is shown and described in Fig. 2A. **B** Comparison of ^{bio}Ub-specific datasets from two experimental repeats.

Figure S3 (to accompany Figure 3)

Immunoblot validations of hits from mitotic exit-specific and non-phase-specific datasets of ubiquitinated proteins. **A** Full size blots from Fig. 3A-B. **B** Additional validations of hits presented in Figure 2: Spartin and NPM1 appear strongly polyubiquitinated in all mitotic fractions, as expected from peptide numbers. (NB Specificity problems with the NPM1 antibody means the polyubiquitinated material may not all be NPM1-specific). KIF2C (MCAK) and RacGAP1 are specifically polyubiquitinated during mitotic exit. Histone H3 is mono-ubiquitinated in M and C1 phases only (this is not consistent with peptide numbers, where C2 > C1, see Supplementary Table S2).

Figure S4 (to accompany Figure 4)

Venus-RacGAP1 destruction during mitotic exit is not significantly altered by assay conditions. **A-B** Venus-tagged RacGAP1 was electroporated into U2OS cells and after 12-24 hours mitotic cells were imaged by fluorescence timelapse microscopy. Venus levels in individual mitotic cells were quantified and plotted as a function of anaphase onset (left-hand panels). The resulting *in vivo* degradation curves are also shown as averaged results with error bars representing standard deviation (right-hand panels). **A** Aurora B inhibitor ZM (10 μM), or DMSO for control cells, was added prior to anaphase onset. **B** Cells were treated with STLC (10 μM) to generate a mixture of monopolar and bipolar spindles at mitosis; all cells were then released into anaphase using ZM treatment.

Figure S5 (to accompany Figure 5)

A Non-degradable KIFC1 localizes prominently on spindle microtubules during mitotic exit. Timelapse images of U2OS cells expressing KIFC1-Venus wild-type (wt-) or

R5A,L8A (nd-) were collected at 3 minute intervals, with DIC images revealing timing of anaphase onset and epifluorescence the localization of KIFC1-Venus. Panels are from cells expressing similar levels of wt- and nd- KIFC1-Venus. Arrows indicate prominent pools of nd-KIFC1-Venus at the spindle poles and central spindle of a cell in telophase, when wt-KIFC1-Venus is no longer strongly visible on the spindle. **B** Spindle pole disassembly during anaphase is delayed in the presence of high levels of KIFC1. Cells prepared as for imaging in **A** were fixed and stained with antibodies against GFP (in green) and β-tubulin (in red), left-hand panel. The distribution of MTs both at the spindle poles, and in the central spindle forming between the separating sister chromatids, was quantified by a single line scan through the axis of the spindle poles of individual anaphase cells, right-hand panels. In cells expressing nd-KIFC1-Venus, tubulin levels were higher at spindle poles than central spindle, relative to -wt cells, in most but not all cells. **C** Expression levels of wt- and nd- KIFC1-Venus in cells analysed in B, measured as total fluorescence over the cell normalized for mean background pixel value. Box and whisker plots show that expression level distributions of the two constructs are almost completely non-overlapping.

Figure S6 (to accompany Figure 5)

A RacGAP1 is selectively targeted for proteolysis outside of the midbody. *In vivo* degradation data from timelapse series in Fig. 4B were reanalyzed to quantify fluorescence levels in the midbody and cytoplasm. Results from one cell are shown in left-hand panel, averaged results in right-hand panel, n=3. Error bars show standard deviations. **B,C** MKLP1 stabilizes Venus-RacGAP1. Venus-tagged RacGAP1 degradation during mitotic exit was measured as described in Fig. 4B. **B** Non-MKLP1-binding Venus-RacGAP1Δ1-52 (ΔN) is degraded more rapidly during mitotic exit than wild-type protein. **C** Venus-tagged RacGAP1 degradation is perturbed in cells co-electroporated with mCherry-MKLP1. **D** Expression levels of mCherry-RacGAP1 wild-type and mutant versions in cells analysed to generate Fig. 5E, with distribution of data in box and whisker plots to show that interquartile ranges are comparable.

Supplemental Movie legends

Supplemental Movies 1 and 2

Timelapse series of U2OS cells filmed 24h after electroporation with Venus-RacGAP1, with cells selected for low-level expression (Supplemental Movie 1) or high-level expression (Supplemental Movie 2). Epifluorescence and DIC images were acquired every 2 minutes using a 40X 1.3 NA OIL objective. Epifluorecence images were collected as 1μm stacks and are shown as maximal projections.

Supplemental Movies 3 and 4

Timelapse series of RPE-α-actinin-Venus cells filmed 24h after electroporation with wild-type mCherry-RacGAP1 (Supplemental Movie 3) or mCherry-RacGAP1-K292R (Supplemental Movie 4). Epifluorescence and DIC images were acquired every 2 minutes using a 40X 1.3 NA OIL objective. Epifluorecence images were collected as 1μm stacks and are shown as maximal projections.

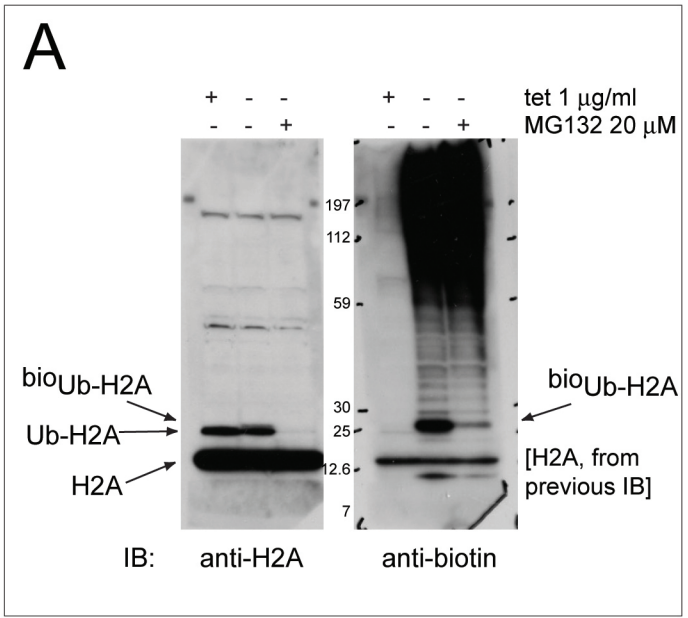
A
+ - -
- - +
tet 1 μg/ml
MG132 20 μM
197
112
59
30
25
12.6
7
bioUb-H2A
Ub-H2A
H2A
bioUb-H2A
[H2A, from previous IB]
IB:
anti-H2A
anti-biotin

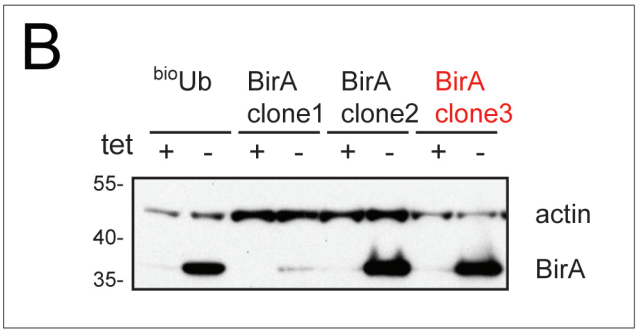
B
bioUb
BirA clone1
BirA clone2
BirA clone3
tet
+ - + - + - + -
55-
40-
35-
actin
BirA

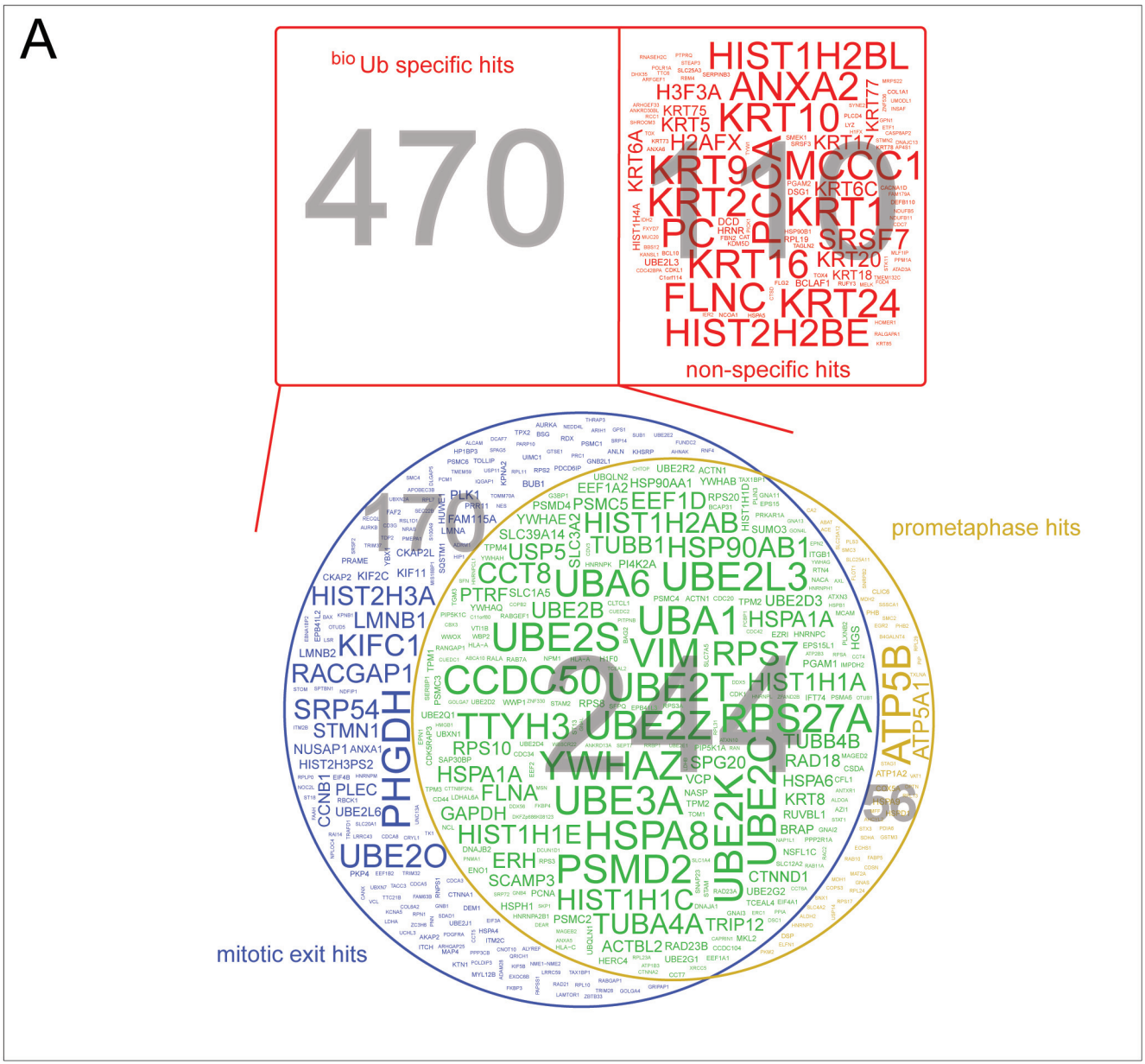
A
bio Ub specific hits
470
non-specific hits
prometaphase hits
mitotic exit hits
150
56
B
124
149
197
Experiment 1
Experiment 2

A

anti-CDC20

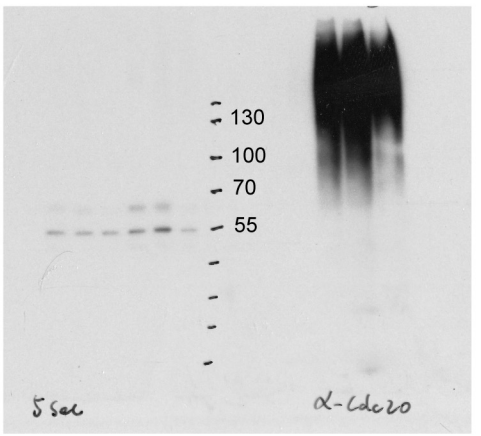

anti-TPX2

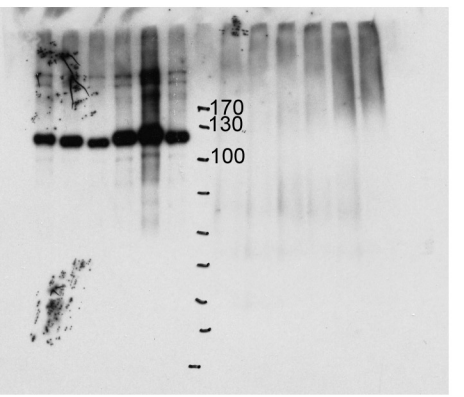

anti-Lamin B2

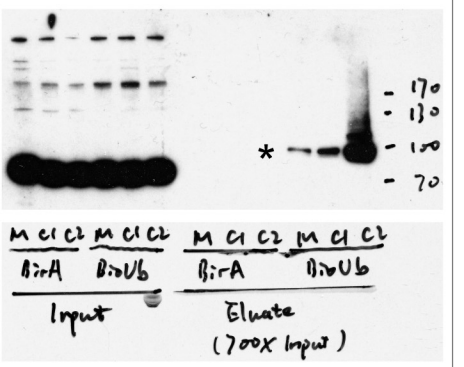

anti-SUG1

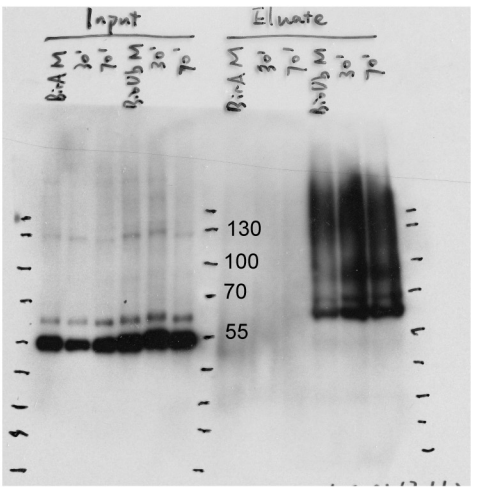

anti-KIF11 (Eg5)

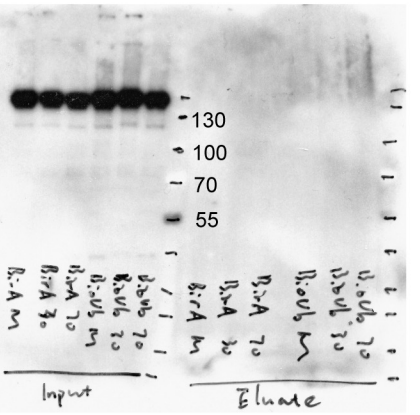

anti-KIFC1 (HSET)

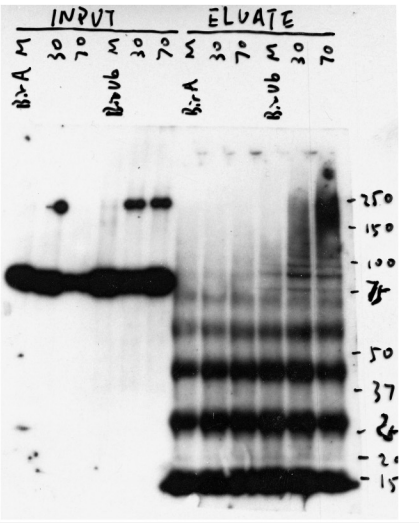

B

anti-spartin

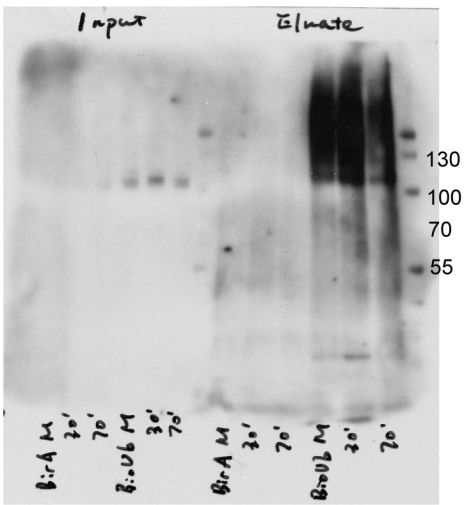

anti-NPM1

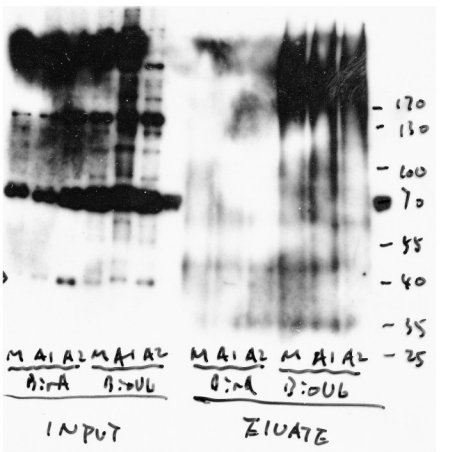

anti-KIF2C (MCAK)

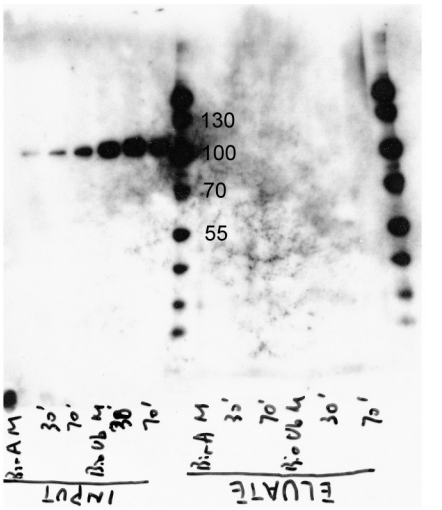

anti-Histone H3

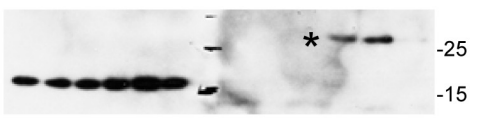

anti-RacGAP1

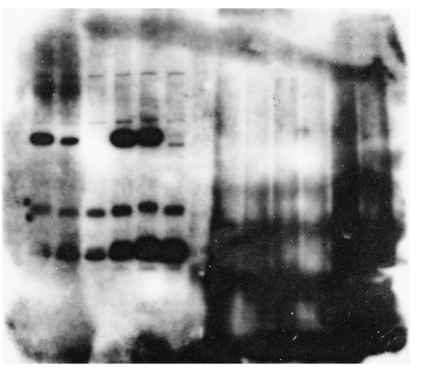

Supplemental Figure S4

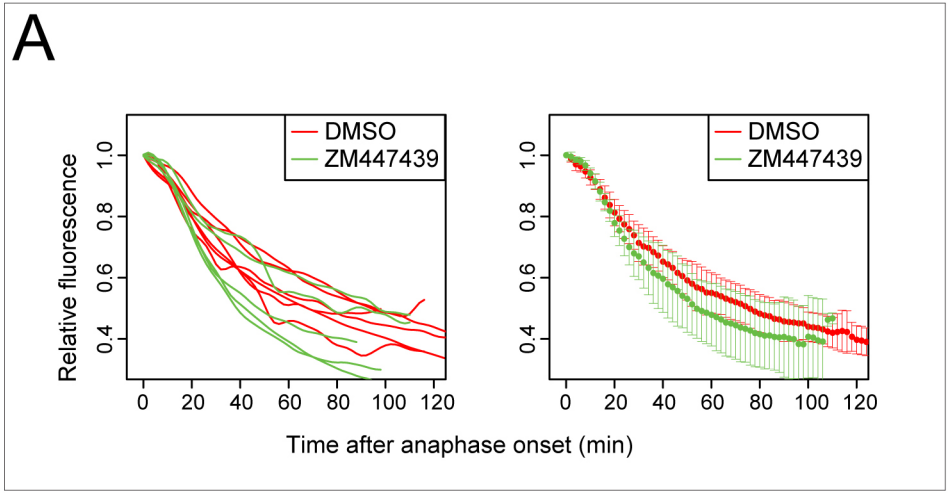

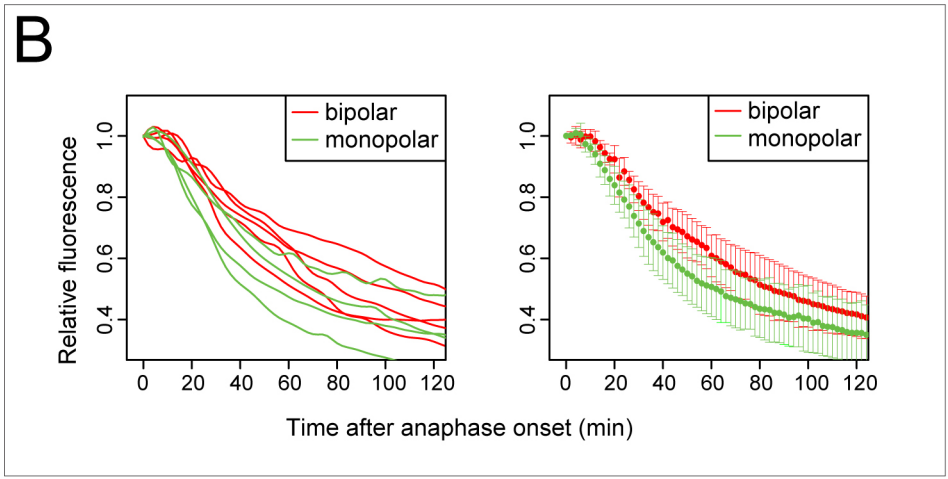

Supplemental Figure S5

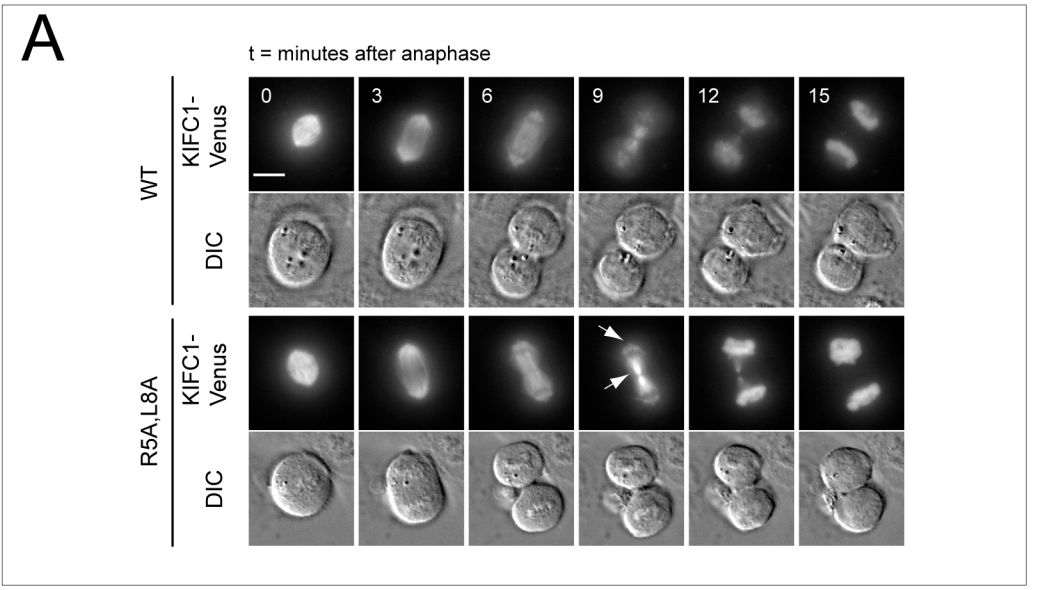

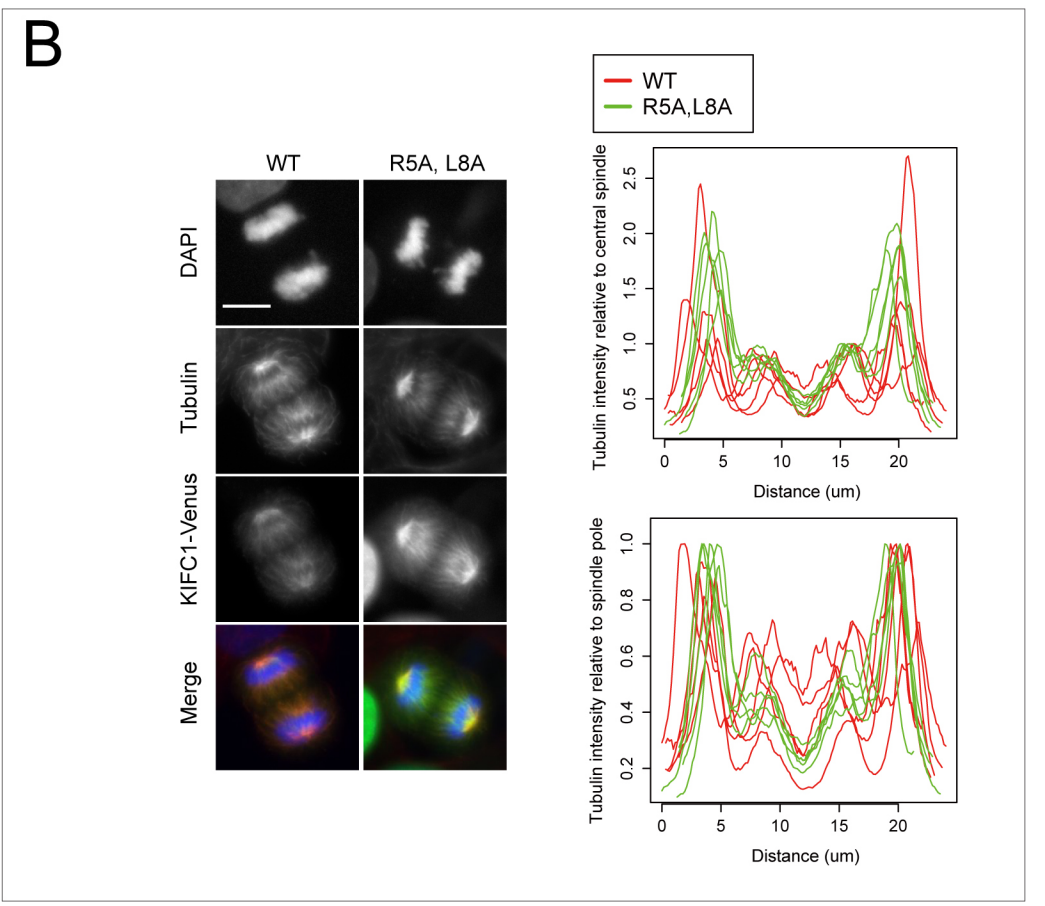

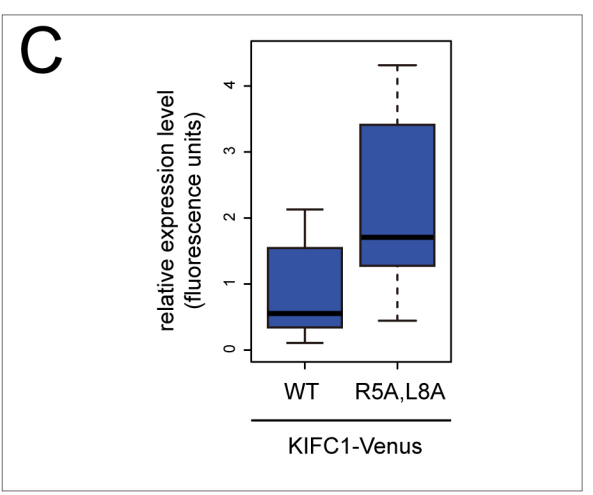

Supplemental Figure S6

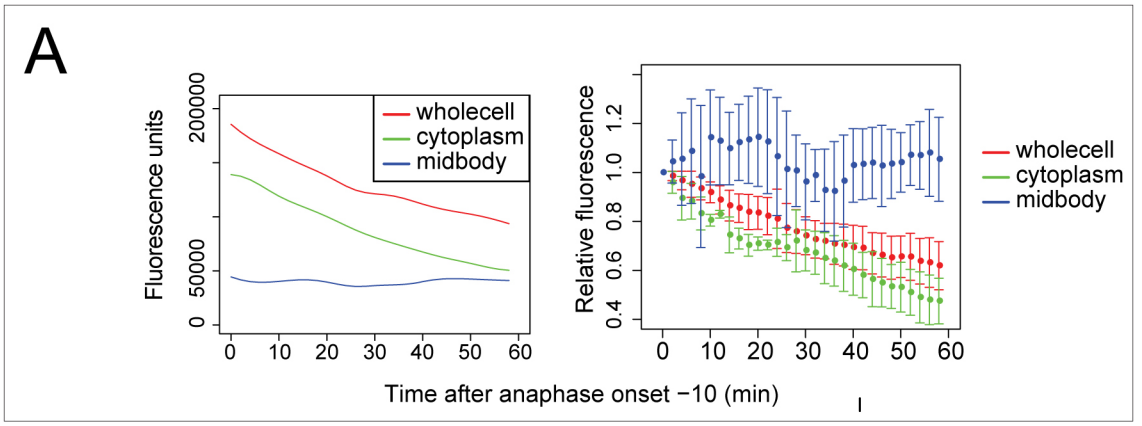

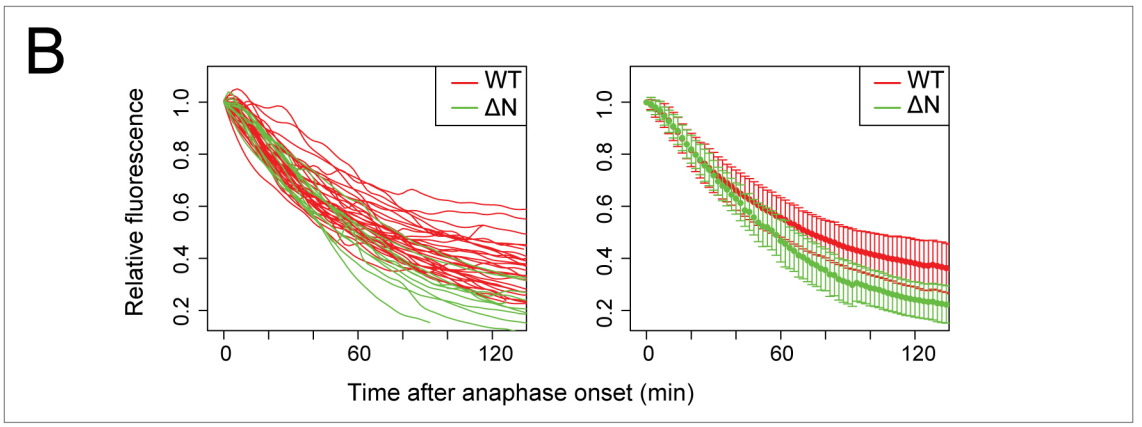

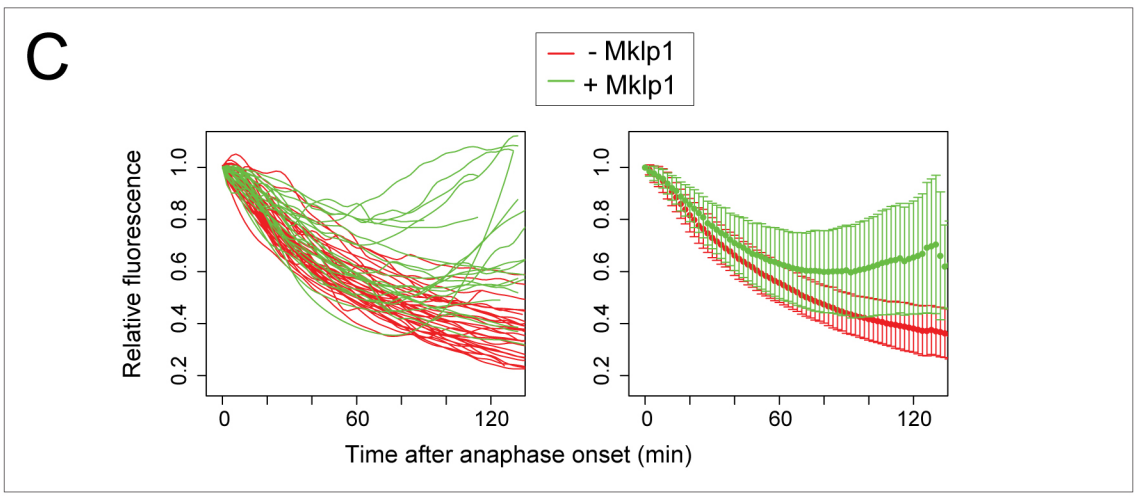

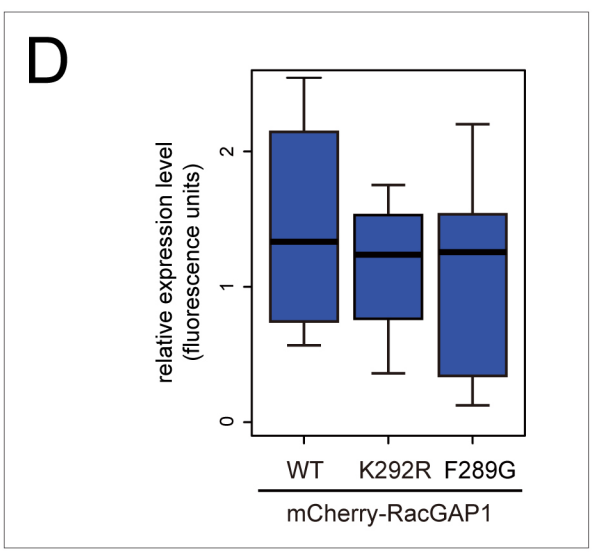

Supplemental Table 3

UPS hits from ^{bio}Ub-specific dataset

classed as anaphase-specific according to peptide numbers from Supplementary Table 2

enzymatic activity		also known as	known specific functions
E1		**Ubiquitin-like modifier-activating enzymes**	
	UBA1		
	UBA6		
E2		**Ubiquitin-conjugating enzymes**	
	UBE2B	HR6B; RAD6B; E2-17kDa	post-replicative DNA damage repair (with RAD18)
	UBE2C	UBCH10	mitotic cyclin destruction
	UBE2D2	UBC4/5B; UBCH4/5B; PUBC1; E2(17)KB2	p53, NFKB signalling (NFKB, TRAF6)
	UBE2D3	UBC5C; UBCH5C	post-replicative DNA damage repair (with RAD18). 'Priming' E2 for NFKB, PCNA
	UBE2D4	UBCH5D	
	UBE2E1	UBCH6	E2 for ISG15 ubiquitin-like modifier
	UBE2E2	UBCH8	
	UBE2G1	UBE2G	
	UBE2G2		ERAD pathways
	UBE2J1		ERAD pathways
	UBE2K	HIP2; LIG	elongating E2, involved in ERAD, NFKB signalling
	UBE2L3	UBCE7; UBCH7	HECT E3-specific E2; K11 in vitro
	UBE2L6	UBCH8	E2 for ubiquitin and ISG15. Involved in p53 regulation
	UBE2N	UBC13; UBCH13; BLU	K63 chains. Involved in NFKB, MAPK signalling, ubiquitinates PCNA
	UBE2O	E2-230K; KIAA1734	
	UBE2Q1	UBE2Q; NICE5	
	UBE2R1	CDC34; UBCH3	SCF-E3-specific E2. K48
	UBE2R2	CDC34B; UBC3B	
	UBE2S	E2EPF	elongating E2, APC/C E3-specific. K11 chains
	UBE2T	HSPC150; PIG50	DNA damage repair, E2 for FANCL E3
	UBE2Z	Use1	charged by UBA6 only
E3		**Ubiquitin-protein ligases**	
	ARIH1	E3 ubiquitin-protein ligase ARIH1	May play a role in protein translation by mediating polyubiquitination of EIF4E2
	CDC20		cell cycle control
	HERC4		probable E3 in protein trafficking
	HUWE1	Hect9; URE-B1	histone ubiquitination, DNA damage repair, p53 regulation
	NDFIP1	NEDD4 family-interacting protein 1	HECT E3 activator
	NEDD4L	NEDD4-like	TGFb signalling inhibition, regulation of plasma membrane channels
	RAD18	RNF73	postreplicative DNA damage repair (with UBE2B), E3 for PCNA K164
	TRIM32	HT2A	HIV1-Tat regulation
	TRIM37		
	TRIP12	ULF	downregulates p19ARF, RNF168 (H2A/H2AX E3)
	UBE3A		signalling pathways, transcriptional coactivator
	RNF4	E3 ubiquitin-protein ligase RNF4;	
	ITCH		inflammatory signaling pathways
	WWP1	NEDD4-like E3 WWP1	TGFb signalling inhibition, regulation of RNF11
other			
	BRAP	BRCA1-associated protein, RNF52	MAPK signalling
	DCAF7	DDB1- and CUL4-associated factor 7	a substrate receptor for CUL4-DDB1 E3 ubiquitin-protein ligase complex
	UBXN1		interacts with the BRCA1-BARD1 heterodimer, and regulates its activity
	UIMC1	BRCA1-A complex subunit RAP80;	
	UBXN2A		
	VCP	Transitional endoplasmic reticulum ATPase; p97	organelle biology, esp ER
	UBXN7	UBX domain-containing protein 7	
DUB			
	OTUB1	Ubiquitin thioesterase OTUB1	specifically remove 'Lys-48'-linked ubiquitin, prevent degradation
	OTUD5	OTU domain-containing protein 5	negative regulator of the innate immune system
	UCHL3	Ubiquitin carboxyl-terminal hydrolase isozyme L3	
	USP11	Ubiquitin carboxyl-terminal hydrolase 11	pathways leading to NF-kappa-B activation, DNA repair
	USP14	Ubiquitin carboxyl-terminal hydrolase 14	proteasome-associated deubiquitinase, regeneration of ubiquitin at proteasome
	USP5	Ubiquitin carboxyl-terminal hydrolase 5	cleaves polyubiquitin, esp. branched chains

Supplemental Table 4 – antibodies used

antibody	from	dilution
Biotin	Cell Signaling (#7075)	1:300
Ubiquitin	Sigma (U5379)	1:100
FK2	Enzo (PW0150)	1:3000
BirA	Abcam (ab14002)	1:1000
Cyclin B1	Abcam (ab11926)	1:1000
Aurora A	BD Biosciences (610939)	1:600
RacGAP1	Abcam (ab2270)	1:1500
KIF11	Jonathon Pines	1:1000
KIF2C	Viji Draviam	1:500
Spartin	Evan Reid	1:500
TPX2	Fanni Gergely	1:1000
CDC20	Bethyl (180A)	1:500
PSMC5	Euromedex (SUG-1B8)	1:2000
LMNB2	Abcam (ab8983)	1:1000
Histone H3	Abcam (ab1791)	1:5000
NPM	Biorbyt (orb6524)	1:1000
UBE2C	Boston Biochem (A-650)	1:200
UBE2R1	Boston Biochem (A-610)	1:200
APC3	Abcam (ab10538)	1:1000
GFP	Abcam (ab290)	1:2000 for immunoblotting
		1:1000 for immunofluorescence
beta-tubulin	Abcam	1:2000
actin	Sigma (A 3853)	1:1000